Fabrication of Slippery Liquid-Infused Coatings in Flexible Narrow-Bore Tubing

Harshit Agarwal,[1] Kayleigh E. Nyffeler,[2,3] Helen E. Blackwell,[2,*] and David M. Lynn[1,2,*]

[1]Department of Chemical & Biological Engineering, University of Wisconsin–Madison, 1415 Engineering Dr., Madison, WI 53706, USA; [2]Department of Chemistry, University of Wisconsin–Madison, 1101 University Ave., Madison, WI 53706, USA; [3]Microbiology Doctoral Training Program, University of Wisconsin–Madison, 1550 Linden Dr., Madison, WI 53706 USA. E-Mail: (H.E.B) blackwell@chem.wisc.edu; (D.M.L) dlynn@engr.wisc.edu

ABSTRACT: We report a layer-by-layer suction-and-flow approach that enables fabrication of polymer-based 'slippery' liquid-infused porous surfaces (SLIPS) in the confined luminal spaces of flexible, narrow-bore tubing. These SLIPS-coated tubes can prevent or strongly reduce surface fouling after prolonged contact, storage, or flow of a broad range of complex fluids and viscoelastic materials, including many that are relevant in the contexts of medical devices (e.g., blood and urine), food processing (beverages and fluids), and other commercial and industrial applications. The robust and mechanically compliant nature of the nanoporous coating used to host the lubricating oil phase allows these coated tubes to be bent, flexed, and coiled repeatedly without affecting their inherent slippery and anti-fouling behaviors. Our results also show that SLIPS-coated tubes can prevent the formation of bacterial biofilms after prolonged and repeated flow-based exposure to the human pathogen *Staphylococcus aureus*, and that the anti-biofouling properties of these coated tubes can be further improved or prolonged by coupling this approach with strategies that permit the sustained release of broad-spectrum antimicrobial agents. The suction-and-flow approach used here enables the application of slippery coatings in the confined luminal space of narrow-bore tubing that is difficult to access using several other methods for the fabrication of liquid-infused coatings, and can be applied to tubing of arbitrary length and diameter. We anticipate that the materials and approaches reported here will prove useful for reducing or preventing bio-fouling, process fouling, and the clogging or occlusion of tubing in a wide range of consumer, industrial, and healthcare-oriented applications.

Keywords: Anti-Fouling, Slippery, Liquid-Infused, Layer-by-Layer, Controlled Release

For Table of Contents Use Only:

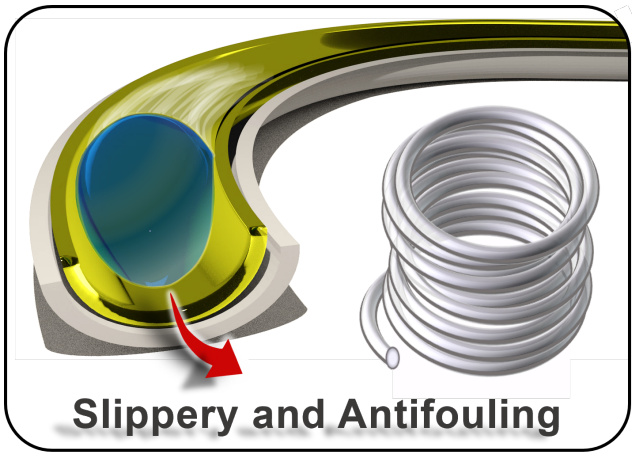

Introduction

Flexible tubing is used to transport liquids and other materials in an enormously broad range of commercial and industrial contexts, but is susceptible to fouling in ways that can be costly in both economic and human terms. Bacterial fouling on the surfaces of indwelling catheters, for example, can lead to systemic infections that are expensive to treat and can be life-threatening, particularly in immunocompromised patients.[1-5] In turn, clotting of blood in venous catheters and arteriovenous shunts can lead to occlusion and result in fatal complications.[3,5-7] More broadly, the fouling of tubing can also lead to contamination, downtime, and high replacement costs in the chemical process industry and in many other healthcare, consumer, and military applications.[8-11] Surface treatments that can kill or prevent the adhesion of microorganisms and keep the surfaces of tubing clear of liquids, viscoelastic solids, or other contaminants thus have the potential to have enormous economic and social impacts. In this paper, we address this challenge and report approaches to the assembly of chemically and mechanically robust anti-fouling coatings in the luminal spaces of narrow-bore tubing used in many biomedical applications and in a variety of other commercial processes.

The work reported here leverages the properties of an emerging class of synthetic and anti-fouling soft materials known as 'slippery liquid-infused porous surfaces' (SLIPS) or 'liquid-impregnated surfaces' (LIS).[12-15] SLIPS and LIS are typically fabricated by the infusion of a lubricating liquid, usually a viscous oil, into a chemically compatible porous or nano/micro-textured host surface.[12,14,16-18] The infused liquid forms a smooth and mobile layer on the surface, resulting in a negligible pinning force and allowing a broad range of substances, including cultures of bacteria and other microorganisms, to simply slide off upon contact.[12-15,19,20] This overall design has been demonstrated to impart several additional practical advantages compared

to other classes of anti-fouling materials, including self-healing properties, high pressure and thermal stability, and good optical transparency.[12-14,21,22] This combination of features has attracted significant levels of interest in the development of SLIPS and LIS as self-cleaning[16,23] and anti-biofouling[13,21,24-27] coatings and as means to endow surfaces with anti-icing,[28,29] anti-corrosion,[30,31] and drag-reducing[32,33] properties. Underscoring their potential practical utility, surfaces and coatings that exhibit slippery behaviors have recently been commercialized to coat the surfaces of containers for the dispensing of commercial liquids and gels and to prevent biofouling in marine environments.

Many different methods have been reported to either modify existing surfaces to render them suitable for the infusion of oils or to fabricate materials with appropriate combinations of roughness, porosity, and chemical functionality that can be applied to other surfaces to impart slippery and anti-fouling properties.[14,15,34] These methods include electrodeposition,[28,35] lithographic patterning,[20,29] polymer-induced wrinkling,[27,36] electro/blow-spinning,[37,38] sol-gel methods,[39,40] chemical vapor deposition (CVD),[41] and layer-by-layer assembly,[42-46] and have enabled the fabrication of SLIPS with vastly different compositions and structures. These techniques are all well suited for the fabrication of SLIPS and LIS on surfaces that are external, exposed, or otherwise readily accessible (e.g., the inner surfaces of wide-mouthed containers). However, most of these methods are inadequate for applying slippery coatings to the inner surfaces of objects with more restricted luminal spaces, including the insides of narrow-bore tubing or the channels of microfluidic devices. As a result, there is only a handful of reports on the fabrication of SLIPS-based coatings on the inside surfaces of flexible tubing.[25,26,41,43,46,47] In one example, Leslie *et al.* reported an approach to fabricate SLIPS on the surface of medical-grade tubing used to design arteriovenous shunts based on the covalent attachment of

perfluorocarbon functionality to the surface, followed by infusion of a fluorinated liquid phase.[25] In another example, MacCallum *et al.* demonstrated an approach to the design of slippery catheter tubing by the direct impregnation of silicone oil into silicone-based tubing.[26] The results of these past studies underscore the potential of liquid-infused coatings to prevent fouling in flexible tubing used in several important biomedical applications and other commercial contexts.

Here, we report a layer-by-layer 'suction-and-flow' approach that can be used to fabricate uniform and conformal polymer-based SLIPS on the luminal surfaces of narrow-bore tubing. This approach can be applied to tubing of arbitrary diameter and length to impart features, including surface and bulk nanoporosity and hydrophobic character that are essential for the subsequent infusion and retention of lubricating oils, increasing the potential for integration of these materials in practical contexts. Moreover, these coatings are physically stable and mechanically robust, permitting them to flex, bend, and survive coiling and other forms of physical manipulation typically experienced by flexible tubing in real-world scenarios. Our results reveal SLIPS-coated tubing to exhibit robust resistance to fouling during the storage or flow of a range of commercial liquids and other substances, as well as prolonged contact with physiological fluids such as blood and urine. Finally, we demonstrate that these slippery coatings maintain anti-fouling properties after ethylene oxide sterilization and that they can be designed to resist the formation of bacterial biofilms for extended periods, either by leveraging their inherent slippery properties or by loading antimicrobial agents that also kill planktonic organisms. When combined, these results provide new pathways toward the fabrication of anti-fouling coatings in flexible tubing used in a broad range of healthcare-oriented applications and other industrial and commercial scenarios in which fouling is endemic.

Materials and Methods

Materials. Polyethyleneimine (Mw ~25,000, Mn ~10,000, branched), acetone, methanol, tetrahydrofuran, acetonitrile, silicone oil (ρ = 0.963 g/mL, η = 45-55 cSt), sodium chloride, calcium chloride, anhydrous magnesium chloride, sodium citrate tribasic dihydrate, sodium sulfate, potassium phosphate monobasic, ammonium chloride, urea, anhydrous creatinine, sodium oxalate, triclosan, and crystal violet (CV) were purchased from Sigma-Aldrich (Milwaukee, WI). Triton X-100 and Tris-HCl were purchased from Promega (Madison, WI). Potassium chloride and PE tubing (1/8″ ID × 1/4″ OD × .062″) were purchased from Fisher Scientific. Phosphate-buffered saline (PBS; 137 mM NaCl, 2.7 mM KCl, 10 mM phosphate; pH 7.4) was prepared from OmniPur 10× concentrate (Millipore Sigma, Milwaukee, WI). Ethanol was obtained from Decon Laboratories (King of Prussia, PA). *n*-Decylamine was purchased from Acros Organics (New Jersey, USA). 2-Vinyl-4,4-dimethylazlactone (VDMA) was a kind gift from Dr. Steven M. Heilmann (3M Corporation, Minneapolis, MN). Poly(2-vinyl-4,4-dimethylazlactone) (PVDMA, MW ≈ 53,000, $Đ$ = 4.1, degree of hydrolysis = 22%) was synthesized by the free-radical polymerization of VDMA, as described previously.[48] Compressed air used to dry samples was filtered through a 0.2 μm membrane syringe filter. Water with a resistivity of 18.2 MΩ was obtained using a Millipore filtration system. Brain heart infusion (BHI) medium was purchased from Teknova (Hollister, CA). Wild-type *S. aureus* (RN6390b; NTCC8325 cured of prophages) was used for all experiments with bacteria.[49] Freshly expired human red blood cells were obtained from the blood bank at the University of Wisconsin Hospital and Clinics. Fresh porcine blood was collected in a 50 mL conical centrifuge tube with 3.4% sodium citrate in PBS at a ratio of 9:1 (blood:citrate) from the Meat Plant located in the

Meat Science & Animal Biologics Discovery Building (UW-Madison, Madison, WI). Lake water was locally sourced from Lake Mendota, Madison, WI. Double India Pale Ale (Double Dog IPA; Flying Dog Brewery) was purchased from a local liquor store (Madison, WI). Tomato ketchup (Simply Heinz, Kraft Heinz Company) and soy sauce (Kroger) were purchased from Pick 'n Save (Madison, WI). Pooled human urine was purchased from Innovative Research Inc. (Novi, MI). Synthetic urine (SU) medium was prepared according to a prior report.[50] The pH was adjusted to 6.0 and the medium was filter-sterilized by passing it through a 0.22 μm pore filter. All materials were used as received without further purification unless otherwise noted. All experiments were performed in triplicate unless otherwise mentioned.

Instrumentation, Data Handling, and General Considerations. Scanning electron micrographs were acquired using a LEO 1550 SEM at an accelerating voltage of 3 kV using an in-lens SEM detector. Coated tubes were sectioned into segments ~1 cm long and then sliced longitudinally to expose the coated luminal surface. Samples were coated with a thin layer of gold using a gold sputterer operating at 10 mA under a vacuum pressure of 50 mTorr for 2 min before imaging. ATR-IR measurements were made using a Bruker Tensor 27 FTIR spectrometer outfitted with a Pike Technologies Diamond ATR stage (Madison, WI), and data were analyzed using Opus Software (version 6.5, Bruker Optik GmbH). Spectra were collected at a resolution of 2 cm^{-1} and are presented as an average of 16 scans. Data were smoothed by applying a nine-point average and baseline-corrected using a concave rubber band correction (10 iterations, 64 points). Digital photographs and videos were acquired using a Samsung Galaxy S8+ smartphone. Contact angle measurements were obtained using a Dataphysics OCA 15 Plus contact angle goniometer at ambient temperature with 2 μL droplets of Milli-Q water. For staining with CV, tubing segments were filled with a 0.1% CV solution in ethanol and incubated for 10 s, and then

the segments were washed with Milli-Q water to remove unbound CV. Droplet sliding times through tubes were measured by placing the desired volume of a water droplet inside a tubing segment held vertically. The time required for the droplet to slide through a predetermined length of the tubing segment was measured using a digital timer. For ethylene oxide (EO) sterilization, multilayer-coated tubing segments (30 cm long, both dry and oil-infused) were sealed in DEFEND self-sealing sterilization pouches and sterilized using a commercial EO sterilization process commonly used to sterilize medical equipment. UV/Vis absorbance values for solutions used to characterize the loading of triclosan were recorded using a Beckman Coulter DU520 UV/Vis spectrophotometer (Fullerton, CA). For measurements of absorbance at 600 nm (OD_{600}) used to monitor bacterial cell growth, 200 μL of cell suspension were added to a clear-bottomed 96-well plate, and absorbance was measured at a wavelength at 600 nm using a Synergy 2 plate reader (Biotek) with Gen5 1.05 software. When OD_{600} was found to be above 1.0, the cell suspensions were diluted accordingly using fresh media until OD_{600} was in a readable range (< 1.0). All numerical data were analyzed using Microsoft Excel for Office 360 and plotted using GraphPad Prism 7 (version 7.0h).

Fabrication of SLIPS-Based Coatings. Tubing segments were cut to desired lengths, cleaned with acetone, dried under a stream of filtered and compressed air, and oxygen plasma-treated for 600 s (Plasma Etch, Carson City, NV). Multilayers were fabricated on the luminal surfaces of the tubing segments by a suction-assisted, flow-based method. Briefly, (i) PEI solution (20 mM in acetone) was pulled up into tubing segments manually by suction using a glass pipette, and the solution was held inside the tubing for 20 s and then forced out; (ii) acetone was pulled up and held inside the tubing for 20 s and then pushed out to rinse the tubing, followed by a second

acetone rinse; (iii) PVDMA solution (20 mM in acetone) was pulled up into the tubing and held inside for 20 s and then forced out, and (iv) tubing was rinsed again using the procedure outlined in step (ii). This cycle was repeated (typically 25 times) to fabricate porous polymer multilayers consisting of the desired number of PEI/PVDMA layer pairs (referred to from hereon as 'bilayers'). The concentrations of the polymer solutions were maintained during assembly by the addition of acetone as needed to compensate for solvent evaporation. After fabrication, multilayers were dried under a stream of filtered, compressed air and used in subsequent experiments immediately or stored in a vacuum desiccator until use. All films were fabricated at ambient room temperature.

Chemical Functionalization of Reactive Multilayers and Infusion of Silicone Oil. Porous polymer multilayer-coated tubing segments containing unreacted azlactone groups, prepared as described above, were filled with solutions of *n*-decylamine (10 mM in THF), reversibly sealed with custom-built metal caps, and then incubated overnight at room temperature. The tubing segments were then rinsed with THF and acetone, dried with filtered air, and placed under vacuum overnight. The resulting hydrophobic multilayer-coated tubing segments were infused with silicone oil by dispensing a desired volume of silicone oil at the top end of a vertical tubing segment and allowing the gravity-driven spreading of the oil from the top to the bottom of the tube. Excess oil was removed by tapping the bottom end of the tubing on a disposable wipe.

Loading and Release of Triclosan. Triclosan was loaded into porous multilayers before the infusion of silicone oil by passing a 1 mL plug of a triclosan solution (200, 500, or 800 mg/mL) in acetone through the multilayer-coated tubing segments (60 cm long). The tubing segments

were then dried under vacuum overnight, cut into 8 cm long segments, and infused with silicone oil as described above. Characterization of the loading of triclosan in these SLIPS-coated tubing segments was performed by stirring triclosan-loaded SLIPS-coated tubing segments in 10 mL methanol at room temperature for 1 hour. The amount of triclosan extracted from the tubing segments into methanol was measured by UV/Vis spectrophotometry at a wavelength of 298 nm and quantified using a standard curve prepared using triclosan in methanol.

Stability Testing of SLIPS-Coated Tubing Segments. All stability tests were performed on tubing segments cut to desired lengths from 60 cm long segments of SLIPS-coated PE (1/8″ ID × 1/4″ OD × .062″) tubes fabricated using the methods described above.

Bending tests: SLIPS-coated tubing segments (30 cm long) were manually bent to form a 180° U-shaped bend ($R_{curvature}$ = 3 cm); the center of the bend was located at the center of the tubing segment. The tubing segment was then straightened out and bent again similarly as described above. This cycle was repeated 500 times.

Shelf-life tests: Tubing segments (30 cm long) coated with multilayer films (both dry and oil-infused) were stored in a coiled state (radius of curvature = 5 cm) at ambient room temperature in the dark for a period of six months.

Stability upon exposure to flow at different shear conditions: SLIPS-coated tubing segments (8 cm long) were connected to a peristaltic pump (Watson-Marlow 120S) with a 3-channel pump head by Tygon tubing segments, and PBS was pumped through the tubing segments at different flow rates (0.5, 6.5, and 12 mL/min) for 7 days at room temperature. The corresponding shear rates were 2.6 s^{-1}, 33.7 $s^{-1,}$ and 62.2 s^{-1} as calculated based on the following equation:[26]

$$\gamma = \frac{4Q}{\pi r^3}$$

where γ is the shear rate (s^{-1}), Q is the volumetric flow rate, and r is the inner radius of the tubing segments.

Contact with complex fluids: SLIPS-coated tubing segments (30 cm long) were filled with citrated whole blood, reversibly sealed with custom-built metal caps, and allowed to sit for two hours. For exposure to synthetic urine, tubing segments were filled with SU medium, custom-built metal caps were used to reversibly seal the ends of the tubing segments, and then the tubing was kept coiled (radius of curvature = 5 cm) at 37 °C for 32 days. For exposure to ketchup, tubing segments were filled and drained (shear rate ≈ 60 s^{-1}) with ketchup 10 times. The sliding times of 20 μL water droplets were measured after each fill and drain cycle.

Characterization of S. aureus adhesion: Freezer stocks of bacteria were maintained at -80 °C in 1:1 BHI:glycerol (50% v/v in Milli-Q water). Wild-type *S. aureus* (RN6390b) from freezer stocks was spread on a BHI agar plate and incubated at 37 °C overnight. The plates were stored at 4–8 °C and used for no more than one week. Prior to each experiment, a single *S. aureus* colony from the plate was suspended in ~10 mL of BHI medium, and the culture was grown overnight at 37 °C with shaking at 200 rpm. To prepare the inoculating subculture of *S. aureus*, the overnight culture was washed three times with BHI containing 1% (w/v) glucose. For washing, the desired volume of *S. aureus* suspension was transferred to sterilized 1.5 mL microcentrifuge tubes and centrifuged at 16,100 × g for 5 min, followed by resuspension of the cell pellet in an amount of fresh BHI containing 1% (w/v) glucose equivalent to the original volume of cell suspension. The final *S. aureus* cell pellet after three washes was resuspended in BHI (+ 1% (w/v) glucose) in an amount equivalent to yield a starting inoculum OD_{600} of 0.23 (~ 10^8 CFU/mL).

For short-term anti-biofouling experiments, SLIPS-coated (with or without triclosan) and uncoated PE tubing segments (1/8″ ID × 1/4″ OD × .062″) were cut to 8 cm long segments and connected to a peristaltic pump with a three-channel pump head (Watson-Marlow 120S) by Tygon tubing segments. Each type of tubing segment (SLIPS-coated, SLIPS-coated + triclosan, and uncoated) was mounted to the peristaltic pump via a different channel, and the ends of the tubing from each channel were immersed into a separate *S. aureus* suspension, prepared as described above. The peristaltic pump was mounted at the top of the incubator, and the tubing segments with *S. aureus* suspensions were positioned inside the incubator at 37 °C. The peristaltic pump was turned on (at 1 mL/min) for 15 mins to fill the entire internal volume of all of the tubing segments and then switched off to hold the *S. aureus* suspension inside the tubing segments to mimic static incubation for 24 hours. The tubing segments were then removed from the incubator and gently washed with DI water to remove any planktonic, non-adhered bacteria from the luminal surface. The edges (~0.5 cm) of each tubing segment were removed, and levels of fouling on luminal surfaces were characterized using a BacTiter-Glo assay (Promega, Madison, WI). Briefly, BacTiter-Glo solution was prepared as described by the manufacturer's protocol, diluted 2× in Milli-Q water, and loaded inside the tubing segments. The tubing segments were incubated for 5 min in the dark at room temperature. Aliquots of BacTiter-Glo solution from the tubing segments (25 μL) were mixed with 25 μL of sterile water in a clear-bottomed white 96-well microtiter plate. Luminescence was characterized using a Synergy 2 plate reader (Biotek) with Gen5 1.05 software.

For multiple-challenge experiments, SLIPS-coated and uncoated PE tubing segments (6 cm long; 1/8″ ID × 1/4″ OD × 0.062″) were incubated at 37 °C and connected to a peristaltic pump by Tygon tubing segments. Each type of tubing segment (SLIPS-coated and uncoated) was

mounted to the peristaltic pump via separate channels, and the ends of the tubing from each channel were immersed into separate *S. aureus* suspensions. Tubing segments were then challenged by pumping *S. aureus* suspensions for 24 h at 1 mL/min (equivalent to a shear rate of 15 s^{-1}). Three SLIPS-coated and uncoated tubing segments were then removed from the incubator and gently washed with DI-water to remove planktonic, non-adherent cells. The ends (~0.5 cm) of each tubing segment were removed, and fouling on the luminal surface was characterized using the BacTiter-Glo assay as described above. The remaining tubing segments in the incubator were washed with PBS at 1 mL/min and then challenged again with fresh *S. aureus* suspension for another 24 h. The tubing segments were challenged with *S. aureus* in this manner at time points of 0, 3, 6, and 10 days (see main text for additional discussion). Fresh uncoated tubing segments were utilized for each *S. aureus* challenge.

Hemolysis assays: Hemolysis assays were performed using a previously reported protocol[51,52] with minor modifications. Briefly, human red blood cells (hRBCs) were washed with Tris-buffered saline (TBS, 10 mM Tris-HCl, 100 mM NaCl, pH 7.5) until clear supernatant was obtained (at least three washes). Aliquots of 400 μL of 1% hRBCs in TBS were loaded into SLIPS-coated and uncoated PE tubing segments (8 cm long). The tubing segments were reversibly sealed with custom-built metal caps leaving ~0.5 cm air gaps on both ends to prevent any interaction of the hRBCs with the metal caps. Tubing segments were then incubated at 37 °C for three hours. Triton X-100 (0.1% w/v) served as the positive lysis control and TBS as a negative lysis control. After incubation, the hRBCs solution inside the tubing segments was transferred to microcentrifuge tubes and centrifuged at 1800g for 5 min. Supernatants (50 μL) were transferred into a 96-well UV microplate and all wells were diluted 2x with 50 μL TBS.

Absorbance was measured at 405 nm using a Tecan M200 multiwell plate reader. The percent of hemolysis was calculated as:

$$Hemolysis\ (\%) = \frac{(A_{405}^{sample} - A_{405}^{negative\ control})}{(A_{405}^{positive\ control} - A_{405}^{negative\ control})} \times 100$$

where 'A_{405} negative control' and 'A_{405} positive control' are the average absorbance values at 405 nm of the 1% hRBCs (in TBS) and 1% hRBCs in (0.1% w/v Triton X-100 in TBS), respectively.

Platelet adhesion assays: Anticoagulated blood, immediately after collection, was transferred into 15 mL conical centrifuge tubes and centrifuged at 200g for 15 min. The platelet-rich plasma (PRP) portion was collected carefully with a pipet so as not to disturb the buffy coat. Calcium chloride (250 mM in Milli-Q water) was added to the platelet solution to achieve a final concentration of 1 mM. Before the platelet adhesion assay, 30 cm long sections of PE tubing segments (SLIPS-coated and uncoated) were washed by passing 1.5 mL of Milli-Q water through the tubing segments. Each tubing segment was then filled with 1.5 mL of calcified PRP and reversibly sealed with custom-built metal caps leaving ~0.5 cm air gaps on both ends to prevent any interaction of calcified PRP with the metal caps. Tubing segments were then incubated at 37 °C for 1.5 hours. Following incubation, the calcified PRP was drained out of the tubing segments, and tubing segments were then gently washed with PBS (500 μL) to remove non-adherent platelets from the luminal surface. The degree of platelet adhesion was determined by measuring the lactate dehydrogenase (LDH) released when the adherent platelets were lysed with Triton-PBS buffer (2% v/v Triton-X-100 in PBS) using a Pierce LDH cytotoxicity assay kit (Thermo Scientific, Fitchburg, WI). The ends (~1 cm) of each tubing segment were removed, and the tubing segments were then filled with Triton-PBS buffer (1.5 mL), reversibly sealed, and incubated at 37 °C for one hour. After incubation, 50 μL volumes of solution from each tubing

segment was transferred into a 96-well UV microplate, and 50 μL of the cytotoxicity assay reagent mixture (prepared as prescribed by the manufacturer; Pierce LDH cytotoxicity assay kit) was added to each well. The plate was left at room temperature in the dark for 30 min, and then absorbance was measured at 490 nm using a Tecan M200 multiwell plate reader.

Results and Discussion

Reactive layer-by-layer assembly of SLIPS in flexible tubing using a suction-and-flow approach

We previously reported a reactive layer-by-layer approach to the design of nanoporous polymer multilayers that is suitable for the fabrication of SLIPS inside narrow-bore (~850 μm diameter) plastic tubing.[45,46] That approach exploited reactions between poly(ethyleneimine) (PEI) and poly(2-vinyl-4,4-dimethylazlactone) (PVDMA, an azlactone-containing polymer that readily reacts with primary amine functionality) and methods for the repetitive and alternating immersion of objects into bulk polymer solutions that are well-suited for coating small segments of tubing (e.g., ~4 cm in length) that are able to fill and drain readily when submerged (Figure 1A). Those immersion-based methods are, however, difficult, impossible, or impractical for coating the insides of longer lengths of tubing (e.g., on the scale of meters or hundreds of meters). To advance processes useful for fabricating nanoporous coatings in tubing of arbitrary length, we developed a 'suction-and-flow' approach (Figure 1B) that uses the intermittent application of negative and positive pressure to alternately draw and then expel solutions of polymer into and from tubing segments. This approach is conceptually straightforward, easy to implement, and can, in principle, be applied to tubing of any desired diameter or length because it only requires access to the two ends of the tubing to draw and expel polymer solutions.

Although this suction-and-flow approach is easy to implement, it was not clear at the outset of these studies whether this approach could be used to fabricate uniform coatings or, more importantly, to recapitulate levels of multilayer roughness and nanoporosity that arise during iterative immersion into bulk polymer solutions needed to design robust SLIPS. To explore the feasibility of this approach, we conducted a series of initial experiments using 60 cm long segments of polyethylene tubing (PE; 1/8″ ID) and solutions of PEI and PVDMA in acetone. The formation of multilayers on the luminal surfaces of these tubing segments was evident from increases in the opacity of the tubing segments as a function of the number of PEI

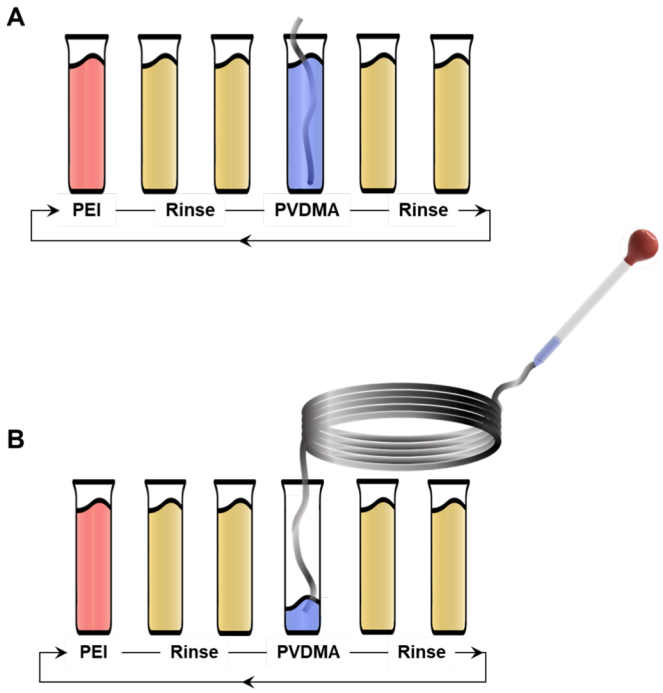

Figure 1. Schematic showing (A) a dipping/immersion-based layer-by-layer approach and (B) the suction-and-flow-based approach used in this study to fabricate polymer multilayers on the luminal surfaces of flexible tubing segments. Instead of submerging shorter flexible tubing segments iteratively into polymer solutions, suction-and-flow methods permit polymer solutions to be iteratively pulled up into and pushed out of coils of tubing of arbitrary length.

and PVDMA layers deposited (each layer pair of PEI and PVDMA deposited during one fabrication cycle is referred to from hereon as constituting one 'bilayer'; see Methods for additional details). Figure 2C shows a length of tubing coated with a film 25 bilayers thick that was stained with the dye crystal violet (CV), which adsorbs strongly to these PEI/PVDMA films. Inspection of this image reveals the presence of continuous color along the length of the tubing, consistent with the presence of a uniform and conformal film on the luminal surface. The uniformity of these coatings persisted, without the formation of visible defects, upon repeated bending and flexing of the tubing, providing a preliminary indication of mechanical durability (data not shown; additional characterization of the ability of these coatings to withstand physical manipulation is included in sections below). Figure 2A–B shows representative top-down SEM

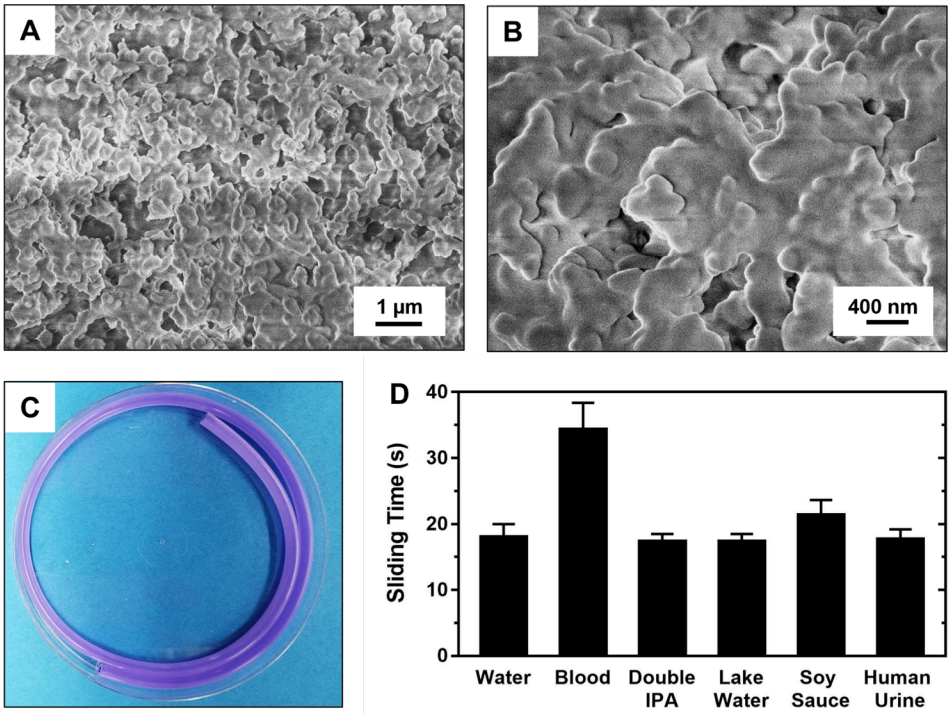

Figure 2. A-B) Representative low and high magnification SEM images of 25-bilayer PEI/PVDMA multilayers coated inside PE tubing segments using the suction-and-flow method. The tubing segments were sliced longitudinally prior to imaging. C) Photo showing a multilayer-coated PE tubing segment stained with CV solution. D) Plot showing the sliding times of 20 µL droplets of various liquids through SLIPS-coated tubing segments 60 cm long.

images of longitudinally sliced sections of multilayer-coated tubing, and reveals evidence of both microscale (Figure 2A) and nanoscale (Figure 2B) roughness and porosity in these coatings (additional images of coatings fabricated in smaller-diameter tubing are included in Figure S1). This morphology was preserved, qualitatively, along the entire length of the coated tube and is generally consistent with nano-and micro-scale roughness observed in PEI/PVDMA multilayers fabricated by immersion-based procedures reported previously.[45,46] Additional characterization of cross-sections of these coatings revealed coatings fabricated using this suction-and-flow method to be substantially thicker (14 ± 3 μm for coatings consisting of 25 bilayers) than those fabricated using immersion-based methods (3.5 ± 0.9 μm for coatings consisting of 35 bilayers).[45]

After fabrication, these reactive coatings were chemically functionalized by infusion with solutions of *n*-decylamine. Figure S2 of the Supporting Information shows the carbonyl region of the IR spectrum of 25-bilayer PEI/PVDMA coatings prior to and after modification with *n*-decylamine, and reveals that the peak at 1826 cm^{-1}, which corresponds to the carbonyl group of unreacted azlactone functionality, to decrease significantly after treatment with *n*-decylamine, consistent with post-fabrication covalent modification of the coating with this hydrophobic amine. Treatment with *n*-decylamine imparted superhydrophobic character to these materials, with a substantial reduction in the contact angle hysteresis of water droplets on the luminal surfaces of the tubing segments, from 46° ± 10° (θ_{adv} = 158° ± 2°, θ_{rec} = 112° ± 8°) to 3° ± 2° (θ_{adv} = 156° ± 1°, θ_{rec} = 152° ± 1°; values are averages of multiple measurements made along the 60 cm length of the coated tubes).

These superhydrophobic tubing segments could be readily infused with silicone oil (see Methods), resulting in improved transparency similar to that of uncoated tubing segments and

slippery character throughout the length of the tubing. We characterized the slippery behavior of the coatings fabricated inside tubes by placing 20 μL water droplets (containing food coloring dye to aid visual inspection) at an open end of tubes held at a tilt angle of 90° and measuring the time required for those droplets to slide through the tube unaided over a specified distance. Figure 2D show that water droplets slid through SLIPS-coated tubing segments 60 cm long in ~16 s (see Video S1). These SLIPS-coated tubing segments were also stable and remained slippery in contact with a range of other complex fluids, including blood, beer, lake water, soy sauce, and human urine (Figure 2D; also refer to Video S2). Apart from blood, which slid more slowly (over ~35 s), droplets of these liquids were observed to slide through the SLIPS-coated tubing segments at similar times (~20 s). In contrast, droplets of these fluids got stuck inside uncoated control tubing segments; see Video S3) and did not move through the tubes without the aid of an external force. Finally, as an initial indicator of anti-biofouling performance, we incubated tubing filled with inocula of the bacterial pathogen *S. aureus* at 37 °C for 24 hours (see Methods). SLIPS-coated tubing segments exhibited a 96 ± 2% reduction in bacterial biofilm formation relative to levels observed in bare, uncoated tubing segments. Additional and more challenging anti-biofouling experiments are discussed in greater detail in the sections below.

The suction-and-flow method used here is well suited for the fabrication of SLIPS on the luminal surfaces of tubing segments of arbitrary size and composition. For these proof-of-concept studies, we coated tubing comprised of polyurethane, polyethylene, glass, and stainless steel with lengths up to one meter and internal diameters ranging from 0.9–3.2 mm (see Figure 3; additional images of a water droplet sliding through a 1-meter-long SLIPS coated tube are shown in Figure S3). Our results show that this suction-and-flow approach can be used to impart anti-fouling and slippery properties to the luminal spaces of various objects including, catheters,

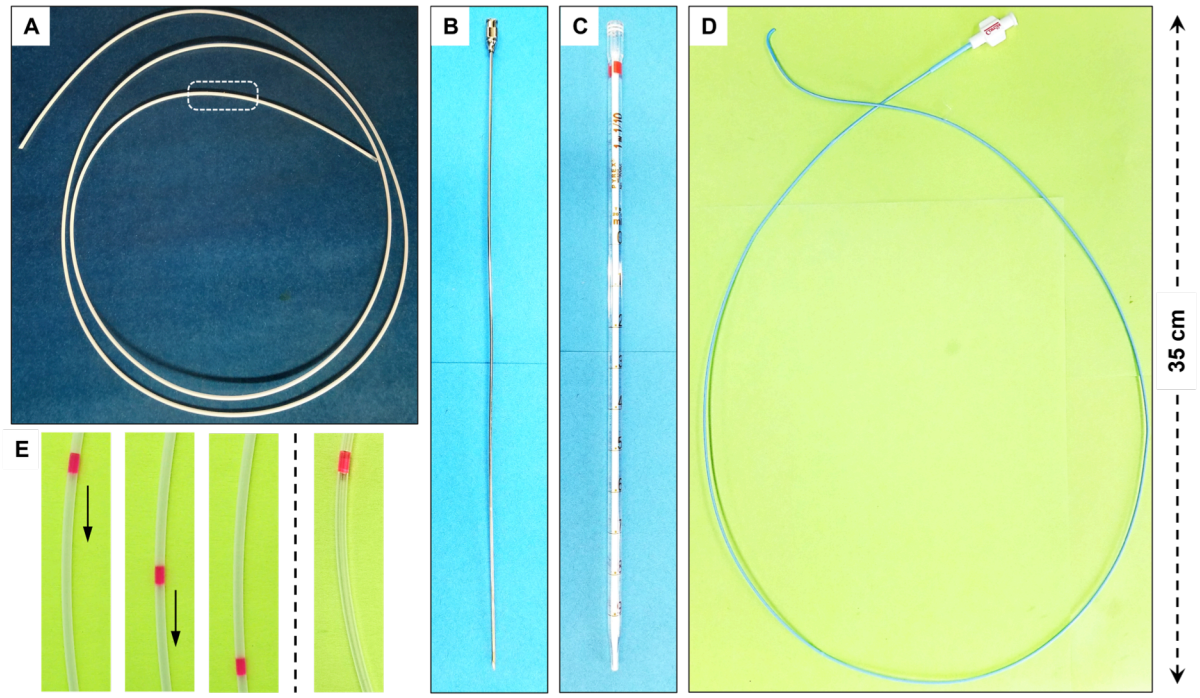

Figure 3. Images showing PEI/PVDMA film-coated tubing and devices of different lengths, diameters, and materials. A) 1 meter long length of coated PE tubing, (B) 32 cm long stainless-steel film-coated syringe needle (1.651 mm ID × 1.194 mm OD), (C) coated 32 cm glass pipette, and (D) coated 4-French catheter (90 cm long). After infusion with silicone oil, all tubing segments were slippery, with 20 µL droplets of Milli-Q water sliding through unaided at times of 32 ± 3, 9 ± 1, 10 ± 2, and 45 ± 5 s, respectively. Water droplets remained stuck inside uncoated tubing segments in each case. E) Time-series images (left of the dotted line) showing sliding of water droplets inside the marked region of the tube (dotted box) shown in (A). Note that tubes become significantly more transparent (similar to that of uncoated tubing segments) after infusion with oil. The water droplets remained stuck inside an uncoated tube (E, right of the dotted line).

needles, pipettes, and other objects that are commonly used to store, transport, and dispense a wide range of fluids and viscoelastic solids. Based on prior reports on immersion-based methods for the fabrication of PEI/PVDMA multilayers,[45,53] we used acetone as the solvent to dissolve the polymers for most of the studies reported here. We note, however, that it is possible to obtain nanoporous coatings and fabricate SLIPS inside tubing using a range of other organic solvents, including *N,N*-dimethylformamide, acetonitrile, and dichloromethane, broadening the range of tubing types to which these slippery coatings can be applied. The results of additional experiments described below demonstrated that these SLIPS coatings remained intact and slippery after exposure to various forms of physical manipulation and chemical exposures commonly experienced by tubing segments in practical scenarios.

Stability and anti-fouling properties of SLIPS-coated polymer tubing upon physical and mechanical manipulation

We found that flexible segments of SLIPS-coated polymer tubing retained their slippery properties after a controlled sequence of repeated bending and coiling. Figure 4A shows a plot of the sliding times of water droplets (20 μL) in SLIPS-coated tubing segments tilted at 90°, measured after a predetermined number of bending cycles (see Figure 4A for the image of a single bend and the Methods section for additional details). The sliding time did not change substantially after up to 500 bending cycles. After 500 cycles, tubing segments were stripped of infused oil by washing with copious amounts of acetone and stained with CV (see Methods). We did not observe cracks, bare spots, or other evidence of the loss of the multilayer coatings in the manipulated portions of the tubing by visual inspection (Figure S4A-C). SLIPS-coated tubing could also be stored in the coiled state for at least six months without loss of functional

properties, such as slippery character (Figure 4B) or anti-biofouling performance. SLIPS-coated tubing segments stored 'on the shelf' for six months exhibited a 95 ± 4% reduction in bacterial biofilm formation relative to levels observed in bare, uncoated tubing segments. This level of

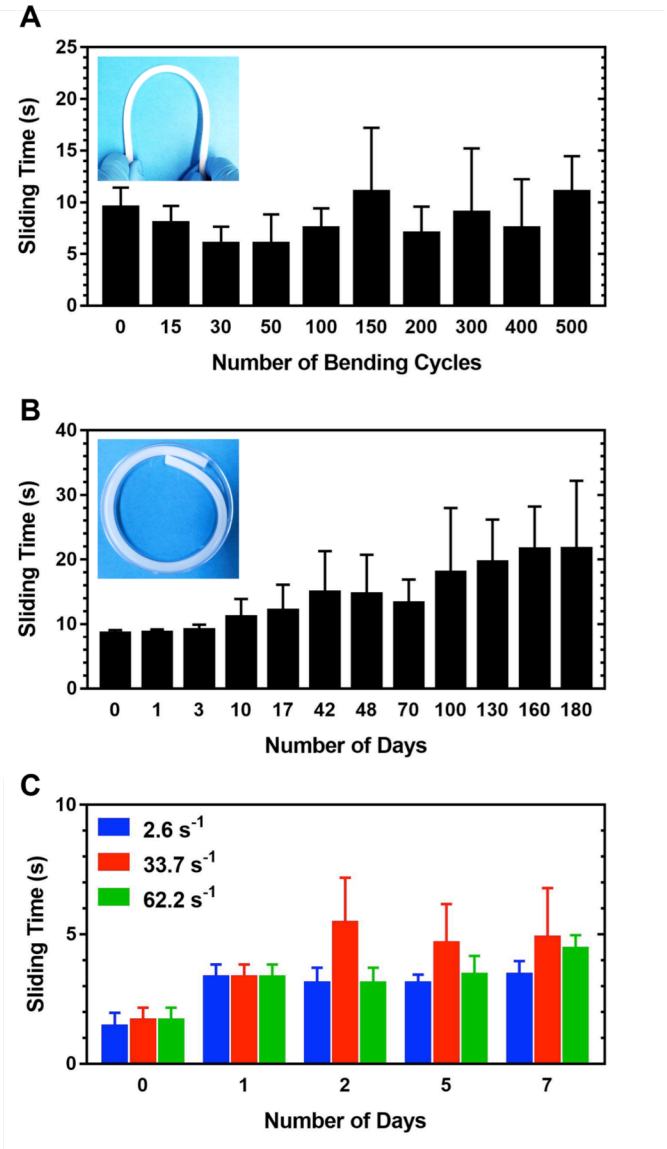

Figure 4. (A) Plot showing sliding times of water droplets through 30 cm long SLIPS-coated PE tubing segments versus the number of repeated bending cycles. The inset shows a representative photo of a single bend (see Methods). (B) Plot showing sliding times of water droplets through 30 cm long SLIPS-coated PE tubing segments as a function of the number of days of coiled shelf storage; the radius of the coil was 5 cm. (C) Sliding times of water droplets through 8 cm long SLIPS-coated PE tubing segments versus days of exposure to flow at three different shear rates (2.6, 33.7, and 62.2 s^{-1}). All sliding time measurements were performed using 20 μL water droplets and the tubing segments were tilted at 90°. Water droplets did not slide through the uncoated (control) tubing segments.

reduction was similar to those measured for 'freshly prepared' SLIPS-coated tubing segments (96 ± 2% reduction in biofilm) under otherwise identical conditions, as described above.

Tubing segments coated with nanoporous PEI/PVDMA multilayers could also be stored 'dry', in the absence of infused oil, for up to six months and then infused with oil immediately prior to use without erosion of functional properties. These coatings remained superhydrophobic (θ_{adv} = 153° ± 1°, and θ_{rec} = 151° ± 1°) under these conditions without any observable cracking or peeling. Infusion of silicone oil resulted in SLIPS-coated tubing with slippery and anti-biofouling properties similar to those described above for SLIPS-coated tubes stored in the oil-infused state (e.g., 97 ± 2% reductions in biofilm formation, relative to uncoated tubing segments, after incubation with cultures of *S. aureus* for 24 hours).

The results of additional experiments demonstrated that SLIPS-coated tubing segments retained their anti-fouling properties upon prolonged exposure to the continuous flow of liquids. We passed PBS through SLIPS-coated tubing at three different shear rates (2.6 s^{-1}, 33.7 s^{-1}, and 62.2 s^{-1}) for seven days to characterize stability under different flow conditions (see Methods for additional details and corresponding flow rates). At predetermined time points (0, 1, 2, 5, and 7 days), tubing segments were removed from flow and characterized for slippery character by measuring the sliding times of water droplets, as described above. SLIPS-coated tubing segments remained slippery at all three shear conditions, with sliding times increasing from ~1.5 s to ~5 s over the first day and then remaining stable for the remaining six days (Figure 4C; segments used in these experiments were 8 cm long). After seven days, the tubes used in these experiments were incubated with *S. aureus* inocula; tubing segments exposed to all three shear rates showed robust anti-fouling performance (96 ± 5%, 96 ± 6%, and 97 ± 3% reductions in biofouling for tubing segments exposed at shear rates of 2.6 s^{-1}, 33.7 s^{-1}, and 62.2 s^{-1}, respectively, relative to

levels observed in bare, uncoated segments). We note that conditions tested here were selected to represent low-shear conditions in the range of those likely to be experienced in indwelling urinary catheters, microfluidic devices, and many food processing applications.[26,54-56] In combination with shear rates, the functional stability of these SLIPS is likely to also depend generally upon the physicochemical properties of the material being transported through the tube, as has been demonstrated for other oil-infused materials in different contexts (the stability of these SLIPS-coated tubes on exposure to a broader range of complex fluids and flow conditions is further discussed below). Finally, we note in the broader context of potential biomedical or food service applications of these materials that these SLIPS-coated tubing segments also retained their slippery and anti-biofouling properties after treatment with ethylene oxide (EO) using commercial procedures commonly used to sterilize medical devices. Of note, EO-sterilized tubes stored on the shelf for ~2 years remained superhydrophobic and demonstrated robust slippery behaviors after infusion with silicone oil (see Figure S5 and surrounding discussion in the Supporting Information for additional results and characterization of EO sterilized tubing).

Functional stability of slippery tubing after prolonged contact and storage with complex fluids

SLIPS-coated tubing remained slippery and anti-fouling after prolonged exposure to a range of chemically complex fluids, including those relevant in medical device-based applications (blood and synthetic urine) and potential food-based applications. Figure 5A shows a segment of SLIPS-coated tubing that was filled and incubated with whole porcine blood for two hours, and then simply tilted to allow the blood to drain from the tube. Visual inspection of this image reveals the inner surface of the tubing to remain free of fouling (a segment of

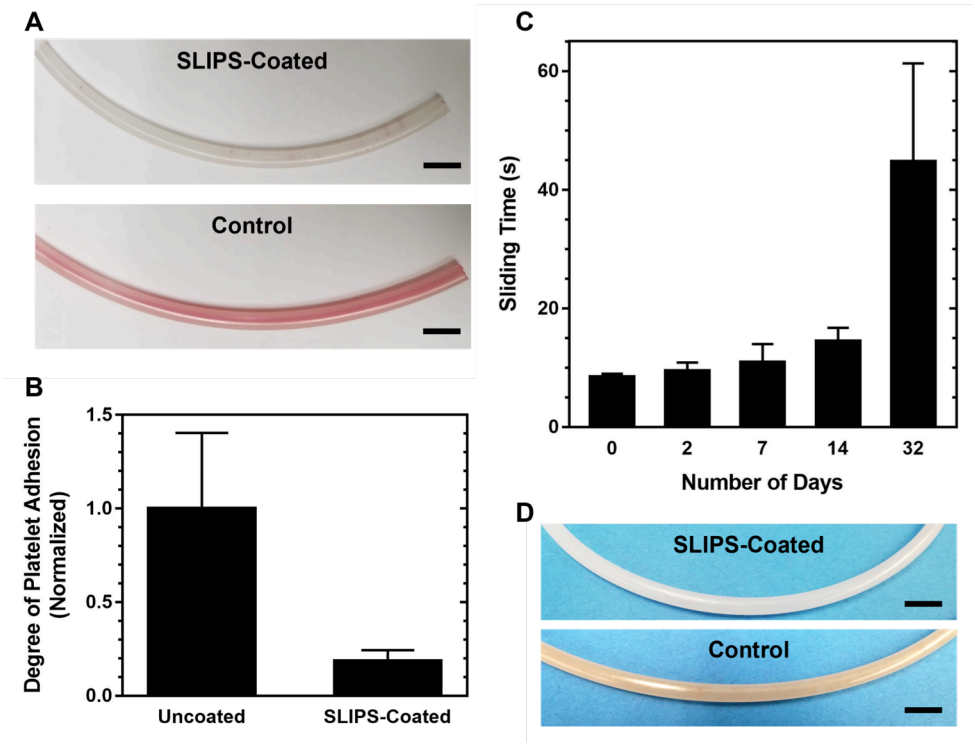

Figure 5. (A) Image showing segments of uncoated (bottom) and SLIPS-coated (top) PE tubing after contact with porcine blood for two hours. (B) Plot showing the degree of platelet adhesion on uncoated and SLIPS-coated tubing segments after incubation with porcine PRP for 1.5 h at 37 °C. The values are normalized with respect to the number of platelets adhered to the uncoated control (see Methods). (C) Plot showing sliding times of water droplets through SLIPS-coated tubing segments 30 cm long versus the number of days of static incubation with synthetic urine. Water droplets (20 µL) were used for sliding time measurements and the tubing segments were tilted to 90°; water droplets did not slide through uncoated tubing segments. (D) Image showing segments of uncoated and SLIPS-coated PE tubing after 10 passes of tomato ketchup (shear rate ≈ 60 s^{-1}; see text). Scale bars are 10 mm.

uncoated and fouled control tubing is also shown for comparison). The ability of SLIPS-coated tubing to prevent fouling by important components of blood involved in clotting and thrombosis was further demonstrated by the results of a platelet adhesion assay, which showed an ~80% reduction in the amount of platelets adherent to the SLIPS-coated tubing relative to uncoated tubing over a period of 1.5 hours (Figure 5B; see Methods for additional details of these experiments). Incubation of SLIPS-coated tubing segments with human red blood cells revealed

them to exhibit outstanding general hemocompatibility, as indicated by a negligible percentage of hemolysis (~0.4% hemolysis; this level was similar to that of uncoated tubing segments (~0.3%) after incubation with red blood cells at 37 °C for 3 hours).

We also performed experiments using synthetic urine to characterize the stability of these SLIPS-coated tubes in high osmolarity chemical environments representative of those encountered during the deployment of urinary catheters. SLIPS-coated tubing segments 30 cm long were filled with synthetic urine, capped and coiled, and then incubated at 37 °C for approximately one month. At predetermined time points, the contents of the tubing were drained and the sliding times of water droplets through the tubing segments were measured. The results of this experiment are shown in Figure 5C and reveal SLIPS-coated tubing to remain slippery after at least a month of exposure to synthetic urine (overall, sliding times increased monotonically over a range from ~8 s to ~44 s over this period, a relatively small change considering that water droplets did not slide at all, without the application of external forces, through uncoated tubing segments). SLIPS-coated tubing segments treated and stored in synthetic urine for one month remained strongly anti-biofouling when incubated in the presence of *S. aureus* (92 ± 4% reduction in biofilm relative to bare, uncoated segments incubated under identical conditions).

In addition to characterization with these important biological fluids, we also performed tests to evaluate the ability of these SLIPS-coated tubes to withstand physical forces and chemical environments experienced in contact with representative food-grade materials. For these experiments, we pushed and pulled tomato ketchup 10 times through a 30 cm long SLIPS-coated PE tubing segment at a shear rate of ~60 s^{-1} (see Methods). Uncoated PE tubing segments were fouled by ketchup in a single pass (Figure 5D, bottom). In contrast, the inner surfaces of

SLIPS-coated tubing segments remained free of residual ketchup even after 10 cycles (Figure 5D, top), and the sliding times of water droplets through these tubing segments increased marginally (from ~9 s to ~45 s over 10 cycles), revealing the robust anti-fouling performance of these materials in the broader context of a potential food processing application.

Characterization of anti-fouling performance upon repeated and longer-term bacterial challenge

We next performed experiments to characterize the anti-biofouling behaviors of SLIPS-coated tubing in more challenging scenarios. To supplement the results of static incubation studies with *S. aureus* described above, we devised a 'serial challenge' experiment, in which SLIPS-coated tubing segments (6 cm long; cut from longer coated segments) were incubated at 37 °C in line with a peristaltic pump, and then periodically challenged by alternately pumping *S. aureus* inocula or PBS through the tubes for 24 h (at a rate of 1 mL/min, corresponding to a shear rate of 5 s^{-1}; these conditions were selected to characterize biofilm formation under low shear and continuous flow conditions representative of those encountered in indwelling urinary catheters).[26,54] After 24 hours in contact with *S. aureus* inocula the tubing segments were pumped continuously with PBS for two to three days and then rechallenged with fresh *S. aureus* inocula for another 24 h (see Methods for additional details of these experiments, and Figure 6A for a visual map showing the timing of these alternating bacterial challenge and wash periods). This cycle was repeated 4 times at 0, 3, 6, and 10 days (Figure 6A). This 'serial challenge' approach was adopted to circumvent limitations associated with the depletion of nutrients (and resulting cell death) that would occur during more prolonged, multiple-day incubation with *S. aureus*.

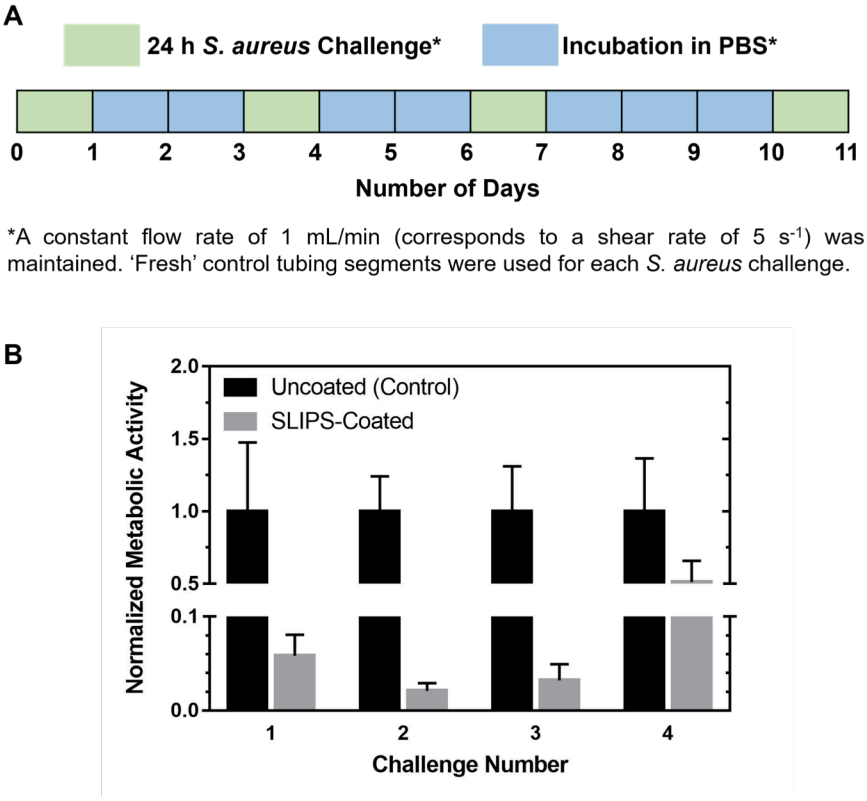

Figure 6. (A) Schematic showing the timing of multi-day bacterial and buffer challenges during flow-based characterization of SLIPS-coated tubes (see text). (B) Plot showing the quantified metabolic activity of *S. aureus* cells associated with the luminal surface of uncoated and SLIPS-coated tubing segments after each of four consecutive 24 h challenges in *S. aureus* inoculum. The values are normalized with respect to the metabolic activity of cells attached to uncoated tubing segments. Metabolic activity measured using BacTiter-Glo; see Methods for full details.

As shown in Figure 6B (gray bars), SLIPS-coated tubing segments remained slippery and retained the ability to substantially prevent *S. aureus* biofilm formation for up to three 24-hour bacterial challenges and seven days of constant flow (black bars indicate levels of biofilm measured on the inner surfaces of bare, uncoated control tubes). After the fourth *S. aureus* challenge, the anti-biofouling performance of SLIPS-coated tubing segments eroded significantly, with an extent of biofouling on the SLIPS-coated tubing segments that was ~50% that of uncoated tubing segments. In addition, these tubing segments were not 'slippery' after the

fourth bacterial challenge, as water droplets stuck to the tubing segments and did not slide without the aid of additional applied forces.

We note that, in a broader context, the multiple challenge experiment described above and summarized in Figure 6 simulates a significantly more demanding biofouling challenge than is likely to be experienced in many practical applications of flexible tubing (e.g., in many healthcare scenarios), as these experiments were performed for extended periods using high-CFU innocula and optimized bacterial growth conditions. Experiments in other simulated environments closer to those that are likely to be found in individual application scenarios would be needed to understand the anti-biofouling performance of these materials, as well as their full range of potential benefits and limitations, in specific applied contexts. In the current context, however, the results of these experiments are significant because they demonstrate that these SLIPS-coated tubes can withstand multiple strong biofouling challenges by this common pathogen for a period of at least one week under a constant flow. We note that the slippery behaviors of these SLIPS-coated tubes could ultimately be manipulated or improved further in the context of specific applications by tuning several design elements, including the thickness of the coatings, the viscosity of the lubricating liquid, or the amount and type of chemical functionalization. In the context of preventing bacterial contamination, we demonstrate below that the anti-biofouling performance of SLIPS-coated tubing can be further improved by incorporating and sustaining the release of a bioactive agent.

Fabrication and evaluation of antimicrobial-loaded SLIPS-coated tubing

We performed a final series of studies to design SLIPS-coated tubing loaded with triclosan, a broad-spectrum small-molecule antimicrobial agent, and further characterize the anti-

biofouling properties of these materials. We reported previously that planar surfaces coated with PEI/PVDMA-based SLIPS can slowly release triclosan into aqueous environments, and that this general approach can, through its ability to kill planktonic cells in surrounding solution, be used to improve the anti-biofouling behaviors of SLIPS when applied to short tubing segments coated using immersion-based approaches.[46] We adapted this approach to load different amounts of triclosan into 60 cm long multilayer-coated PE tubing segments (final loadings were ~300, 500, and 1100 $\mu g/cm^{-2}$; see Figure S6A) using acetone solutions of triclosan at three different concentrations. Additional characterization of the impact of triclosan loading levels on the advancing water contact angle and contact angle hysteresis of the 'dry' multilayer coatings in the tubing segments (i.e., prior to oil infusion) is shown in Figure S6B.

All of the triclosan-loaded tubes were slippery upon initial infusion with oil (water droplets slid through these triclosan-loaded, oil-infused tubes tilted at 90° in ~5 seconds). However, the results of additional experiments involving exposure of these triclosan-loaded tubes to a constant flow of PBS (at 1 mL/min) for extended periods (10 days) revealed that the presence of triclosan can, when loaded at sufficiently high concentrations, lead to changes in multilayer surface properties needed for the stable infusion of silicone oil (Figure S6B,C). While tubes loaded at lower concentrations of triclosan remained slippery and anti-fouling after 10 days of exposure to PBS (Figure S6C,D), droplets in tubes with the highest loading of triclosan became pinned and could no longer slide through unaided (Figure 7A). We note that the loss of slippery character in these tubes was due to the gradual loss of oil, a common failure mode for liquid-infused materials,[15,18] and not due to physical disruption of the coating itself (in these cases, slippery properties could be recovered simply by re-infusion with additional silicone oil). However, these 'sticky' oil-infused tubes were still able to strongly resist the formation of *S.*

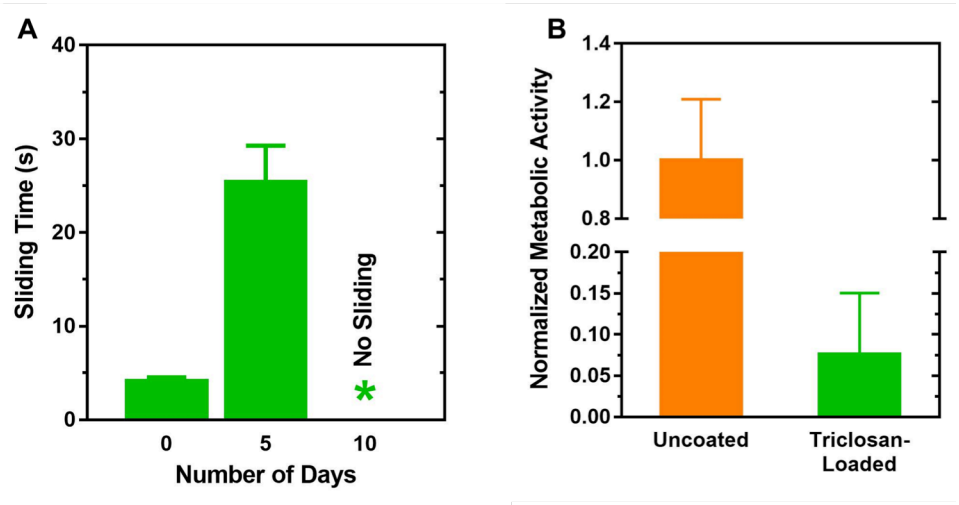

Figure 7. (A) Plot showing droplet sliding times versus the number of days of exposure to flow in SLIPS-coated tubing segments loaded using a 1100 μg/cm^{-2} solution of triclosan (the highest concentration used here; see Supporting Information for additional results and associated results obtained in tubing loaded using lower concentrations of triclosan). After 10 days, tubing segments were subjected to a 24 h static *S. aureus* challenge. Panel (B) shows a plot of normalized metabolic activity of *S. aureus* in these tubing segments incubated with bacteria. Metabolic activity measured using BacTiter-Glo; see Methods for full details.

aureus biofilms. As shown in Figure 7B, these triclosan-loaded segments affected ~94% reductions in biofouling relative to uncoated controls, a level that is statistically indistinguishable from other freshly prepared SLIPS-coated control tubes (no-triclosan; as discussed above). We were unable to quantitatively characterize triclosan release profiles in the narrow-bore tubing under the conditions used in these flow-based experiments, and it is likely that loading and release could be further optimized beyond the proof-of-concept conditions used here. The continued robust anti-fouling behavior observed here is, however, consistent with the continued release of biologically relevant levels of triclosan after loss of slippery character and suggests that the infusion of this antimicrobial agent can be used to offset the effects of gradual oil loss or other related outcomes that reduce the inherent slippery nature of these materials. We conclude that the loading of bioactive agents in these SLIPS-coated tubes can provide a useful strategy to

improve or prolong anti-biofouling performance under conditions, such as prolonged exposure to flow, for which inherent slippery character may be difficult to maintain. These results are broadly consistent with those our initial report on controlled-release SLIPS in static environments[46] and, in combination with other recently-reported strategies (including impregnation of nitric oxide within the bulk,[47,57] incorporation of silver nanoparticles,[58] and covalent immobilization of vancomycin on the underlying porous matrix[59]), provide useful tools to improve or prolong the anti-biofouling performance of SLIPS.

Summary and Conclusions

We have developed a layer-by-layer suction-and-flow approach for fabricating uniform and conformal, SLIPS-based anti-fouling coatings on the luminal surfaces of narrow-bore tubing. The mechanically compliant nature of the nanoporous polymer coating used to host the lubricating oil phase allows these coated tubes to be bent, flexed, and coiled repeatedly, while maintaining the inherent slippery and anti-fouling behaviors. These SLIPS-coated tubes remain clear of surface fouling after the prolonged flow and/or storage of a broad range of complex fluids and viscoelastic gels, including many substances that are relevant in the contexts of medical devices (e.g., catheters, arteriovenous shunts, etc.), food processing, and other commercial and industrial applications. Our results show that these SLIPS-coated tubes can prevent the formation of bacterial biofilms after prolonged and repeated exposure to cultures of *S. aureus*, a notorious human pathogen, under flow conditions, and that the anti-biofouling properties of these coated tubes can be further improved or prolonged by adopting additional strategies that permit the sustained release of a broad-spectrum antimicrobial agent. This approach provides opportunities to fabricate slippery anti-fouling coatings in the confined

luminal space of narrow-bore flexible tubing that is difficult to access using many other methods that are common for the fabrication of SLIPS and LIS, and can be applied to tubing of arbitrary size and length. The materials, techniques, and insights reported here could thus prove useful for reducing or preventing bio-fouling, process fouling, or the clogging and occlusion of tubing in a wide range of consumer, industrial, and healthcare-oriented applications.

Acknowledgments. Financial support for this work was provided in part by the National Science Foundation through a grant provided to the UW–Madison Materials Research Science and Engineering Center (MRSEC; DMR-1720415) and by the UW–Madison Wisconsin Alumni Research Foundation (WARF) through grants provided by the WARF Accelerator Program and the Draper Technology Innovation Fund (Draper-TIF). Bacteriological assay development was supported by the NIH (R35 GM131817 to H.E.B.). K.E.N. was supported in part by the UW−Madison NIH Chemistry-Biology Interface Training Program (T32 GM008505). The authors acknowledge the use of instrumentation supported by the NSF through the UW MRSEC (DMR-1720415). We thank Dr. Angélica de L. Rodríguez López, Prof. Sean P. Palecek, and Dr. Timothy A. Hacker for many helpful discussions.

Supporting Information. Plots, pictures, and videos providing additional characterization of the physicochemical and functional properties of liquid-infused coatings and coated tubes (PDF). This material is available free of charge via the Internet.

ORCID

Kayleigh E. Nyffeler: 0000-0002-1870-6162
Helen E. Blackwell: 0000-0003-4261-8194
David M. Lynn: 0000-0002-3140-8637

References

1. Donlan, R. M. Biofilms and Device-Associated Infections. *Emerging Infect. Dis.* **2001,** *7,* 277-281.

2. Francolini, I.; Donelli, G. Prevention and Control of Biofilm-Based Medical-Device-Related Infections. *FEMS Immunol. Med. Microbiol.* **2010,** *59,* 227-238.

3. Banerjee, I.; Pangule, R. C.; Kane, R. S. Antifouling Coatings: Recent Developments in the Design of Surfaces That Prevent Fouling by Proteins, Bacteria, and Marine Organisms. *Adv. Mater.* **2011,** *23,* 690-718.

4. Campoccia, D.; Montanaro, L.; Arciola, C. R. A Review of the Biomaterials Technologies for Infection-Resistant Surfaces. *Biomaterials* **2013,** *34,* 8533-8554.

5. Zander, Z. K.; Becker, M. L. Antimicrobial and Antifouling Strategies for Polymeric Medical Devices. *ACS Macro Lett.* **2018,** *7,* 16-25.

6. Werner, C.; Maitz, M. F.; Sperling, C. Current Strategies Towards Hemocompatible Coatings. *J. Mater. Chem.* **2007,** *17,* 3376-3384.

7. Wallace, A.; Albadawi, H.; Patel, N.; Khademhosseini, A.; Zhang, Y. S.; Naidu, S.; Knuttinen, G.; Oklu, R. Anti-Fouling Strategies for Central Venous Catheters. *Cardiovasc. Diagn. Ther.* **2017,** *7,* S246-S257.

8. *Marine and Industrial Biofouling*, 1 ed.; Flemming, H.-C.; Murthy, P. S.; Venkatesan, R.; Cooksey, K. E., Eds.; Springer, **2009**.

9. *The Role of Biofilms in Device-Related Infections*, 1 ed.; Shirtliff, M.; Leid, J. G., Eds.; Springer, **2009**.

10. Yao, X.; Song, Y.; Jiang, L. Applications of Bio-Inspired Special Wettable Surfaces. *Adv. Mater.* **2011,** *23,* 719-734.

11. Buskens, P.; Wouters, M.; Rentrop, C.; Vroon, Z. A Brief Review of Environmentally Benign Antifouling and Foul-Release Coatings for Marine Applications. *J. Coat. Technol. Res.* **2013,** *10,* 29-36.

12. Wong, T.-S.; Kang, S. H.; Tang, S. K. Y.; Smythe, E. J.; Hatton, B. D.; Grinthal, A.; Aizenberg, J. Bioinspired Self-Repairing Slippery Surfaces with Pressure-Stable Omniphobicity. *Nature* **2011,** *477,* 443-447.

13. Sotiri, I.; Overton, J. C.; Waterhouse, A.; Howell, C. Immobilized Liquid Layers: A New Approach to Anti-Adhesion Surfaces for Medical Applications. *Exp. Biol. Med.* **2016,** *241,* 909-918.

14. Solomon, B. R.; Subramanyam, S. B.; Farnham, T. A.; Khalil, K. S.; Anand, S.; Varanasi, K. K., Chapter 10 Lubricant-Impregnated Surfaces. In *Non-Wettable Surfaces: Theory, Preparation and Applications*, The Royal Society of Chemistry: 2017; pp 285-318.

15. Villegas, M.; Zhang, Y.; Abu Jarad, N.; Soleymani, L.; Didar, T. F. Liquid-Infused Surfaces: A Review of Theory, Design, and Applications. *ACS Nano* **2019,** *13,* 8517-8536.

16. Lafuma, A.; Quéré, D. Slippery Pre-Suffused Surfaces. *EPL (Europhysics Letters)* **2011,** *96,* 56001.

17. Yao, X.; Hu, Y.; Grinthal, A.; Wong, T.-S.; Mahadevan, L.; Aizenberg, J. Adaptive Fluid-Infused Porous Films with Tunable Transparency and Wettability. *Nat. Mater.* **2013,** *12,* 529-534.

18. Peppou-Chapman, S.; Hong, J. K.; Waterhouse, A.; Neto, C. Life and Death of Liquid-Infused Surfaces: A Review on the Choice, Analysis and Fate of the Infused Liquid Layer. *Chem. Soc. Rev.* **2020,** *49,* 3688-3715.

19. Anand, S.; Paxson, A. T.; Dhiman, R.; Smith, J. D.; Varanasi, K. K. Enhanced Condensation on Lubricant-Impregnated Nanotextured Surfaces. *ACS Nano* **2012,** *6,* 10122-10129.

20. Smith, J. D.; Dhiman, R.; Anand, S.; Reza-Garduno, E.; Cohen, R. E.; McKinley, G. H.; Varanasi, K. K. Droplet Mobility on Lubricant-Impregnated Surfaces. *Soft Matter* **2013,** *9,* 1772-1780.

21. Epstein, A. K.; Wong, T.-S.; Belisle, R. A.; Boggs, E. M.; Aizenberg, J. Liquid-Infused Structured Surfaces with Exceptional Anti-Biofouling Performance. *Proc. Natl. Acad. Sci. U. S. A.* **2012,** *109,* 13182-13187.

22. Daniel, D.; Mankin, M. N.; Belisle, R. A.; Wong, T.-S.; Aizenberg, J. Lubricant-Infused Micro/Nano-Structured Surfaces with Tunable Dynamic Omniphobicity at High Temperatures. *Appl. Phys. Lett.* **2013,** *102,* 231603.

23. Liu, H.; Zhang, P.; Liu, M.; Wang, S.; Jiang, L. Organogel-Based Thin Films for Self-Cleaning on Various Surfaces. *Adv. Mater.* **2013,** *25,* 4477-4481.

24. Xiao, L.; Li, J.; Mieszkin, S.; Di Fino, A.; Clare, A. S.; Callow, M. E.; Callow, J. A.; Grunze, M.; Rosenhahn, A.; Levkin, P. A. Slippery Liquid-Infused Porous Surfaces Showing Marine Antibiofouling Properties. *ACS Appl. Mater. Interfaces* **2013,** *5,* 10074-10080.

25. Leslie, D. C.; Waterhouse, A.; Berthet, J. B.; Valentin, T. M.; Watters, A. L.; Jain, A.; Kim, P.; Hatton, B. D.; Nedder, A.; Donovan, K.; Super, E. H.; Howell, C.; Johnson, C. P.; Vu, T. L.; Bolgen, D. E.; Rifai, S.; Hansen, A. R.; Aizenberg, M.; Super, M.; Aizenberg, J.; Ingber, D. E. A Bioinspired Omniphobic Surface Coating on Medical Devices Prevents Thrombosis and Biofouling. *Nat. Biotechnol.* **2014,** *32,* 1134-1140.

26. MacCallum, N.; Howell, C.; Kim, P.; Sun, D.; Friedlander, R.; Ranisau, J.; Ahanotu, O.; Lin, J. J.; Vena, A.; Hatton, B.; Wong, T.-S.; Aizenberg, J. Liquid-Infused Silicone as a Biofouling-Free Medical Material. *ACS Biomater. Sci. Eng.* **2015,** *1,* 43-51.

27. Ware, C. S.; Smith-Palmer, T.; Peppou-Chapman, S.; Scarratt, L. R. J.; Humphries, E. M.; Balzer, D.; Neto, C. Marine Antifouling Behavior of Lubricant-Infused Nanowrinkled Polymeric Surfaces. *ACS Appl. Mater. Interfaces* **2018,** *10,* 4173-4182.

28. Kim, P.; Wong, T.-S.; Alvarenga, J.; Kreder, M. J.; Adorno-Martinez, W. E.; Aizenberg, J. Liquid-Infused Nanostructured Surfaces with Extreme Anti-Ice and Anti-Frost Performance. *ACS Nano* **2012,** *6,* 6569-6577.

29. Subramanyam, S. B.; Rykaczewski, K.; Varanasi, K. K. Ice Adhesion on Lubricant-Impregnated Textured Surfaces. *Langmuir* **2013,** *29,* 13414-13418.

30. Qiu, R.; Zhang, Q.; Wang, P.; Jiang, L.; Hou, J.; Guo, W.; Zhang, H. Fabrication of Slippery Liquid-Infused Porous Surface Based on Carbon Fiber with Enhanced Corrosion Inhibition Property. *Colloids Surf. Physicochem. Eng. Aspects* **2014,** *453,* 132-141.

31. Tuo, Y.; Zhang, H.; Chen, W.; Liu, X. Corrosion Protection Application of Slippery Liquid-Infused Porous Surface Based on Aluminum Foil. *Appl. Surf. Sci.* **2017,** *423,* 365-374.

32. Solomon, B. R.; Khalil, K. S.; Varanasi, K. K. Drag Reduction Using Lubricant-Impregnated Surfaces in Viscous Laminar Flow. *Langmuir* **2014,** *30,* 10970-10976.

33. Rosenberg, B. J.; Van Buren, T.; Fu, M. K.; Smits, A. J. Turbulent Drag Reduction over Air- and Liquid- Impregnated Surfaces. *Phys. Fluids* **2016,** *28,* 015103.

34. Howell, C.; Grinthal, A.; Sunny, S.; Aizenberg, M.; Aizenberg, J. Designing Liquid-Infused Surfaces for Medical Applications: A Review. *Adv. Mater.* **2018,** *30,* 1802724.

35. Tesler, A. B.; Kim, P.; Kolle, S.; Howell, C.; Ahanotu, O.; Aizenberg, J. Extremely Durable Biofouling-Resistant Metallic Surfaces Based on Electrodeposited Nanoporous Tungstite Films on Steel. *Nat. Commun.* **2015,** *6,* 8649.

36. Yuan, S.; Luan, S.; Yan, S.; Shi, H.; Yin, J. Facile Fabrication of Lubricant-Infused Wrinkling Surface for Preventing Thrombus Formation and Infection. *ACS Appl. Mater. Interfaces* **2015,** *7,* 19466-19473.

37. Abe, J.; Tenjimbayashi, M.; Shiratori, S. Electrospun Nanofiber Slips Exhibiting High Total Transparency and Scattering. *RSC Advances* **2016,** *6,* 38018-38023.

38. Yuan, S.; Li, Z.; Song, L.; Shi, H.; Luan, S.; Yin, J. Liquid-Infused Poly(Styrene-b-Isobutylene-b-Styrene) Microfiber Coating Prevents Bacterial Attachment and Thrombosis. *ACS Appl. Mater. Interfaces* **2016,** *8,* 21214-21220.

39. Kim, P.; Kreder, M. J.; Alvarenga, J.; Aizenberg, J. Hierarchical or Not? Effect of the Length Scale and Hierarchy of the Surface Roughness on Omniphobicity of Lubricant-Infused Substrates. *Nano Lett.* **2013,** *13,* 1793-1799.

40. Wei, C.; Zhang, G.; Zhang, Q.; Zhan, X.; Chen, F. Silicone Oil-Infused Slippery Surfaces Based on Sol–Gel Process-Induced Nanocomposite Coatings: A Facile Approach to Highly Stable Bioinspired Surface for Biofouling Resistance. *ACS Appl. Mater. Interfaces* **2016,** *8,* 34810-34819.

41. Badv, M.; Jaffer, I. H.; Weitz, J. I.; Didar, T. F. An Omniphobic Lubricant-Infused Coating Produced by Chemical Vapor Deposition of Hydrophobic Organosilanes Attenuates Clotting on Catheter Surfaces. *Sci. Rep.* **2017,** *7,* 11639.

42. Huang, X.; Chrisman, J. D.; Zacharia, N. S. Omniphobic Slippery Coatings Based on Lubricant-Infused Porous Polyelectrolyte Multilayers. *ACS Macro Lett.* **2013,** *2,* 826-829.

43. Sunny, S.; Vogel, N.; Howell, C.; Vu, T. L.; Aizenberg, J. Lubricant-Infused Nanoparticulate Coatings Assembled by Layer-by-Layer Deposition. *Adv. Funct. Mater.* **2014,** *24,* 6658-6667.

44. Manabe, K.; Kyung, K.-H.; Shiratori, S. Biocompatible Slippery Fluid-Infused Films Composed of Chitosan and Alginate Via Layer-by-Layer Self-Assembly and Their Antithrombogenicity. *ACS Appl. Mater. Interfaces* **2015,** *7,* 4763-4771.

45. Manna, U.; Lynn, D. M. Fabrication of Liquid-Infused Surfaces Using Reactive Polymer Multilayers: Principles for Manipulating the Behaviors and Mobilities of Aqueous Fluids on Slippery Liquid Interfaces. *Adv. Mater.* **2015,** *27,* 3007-3012.

46. Manna, U.; Raman, N.; Welsh, M. A.; Zayas-Gonzalez, Y. M.; Blackwell, H. E.; Palecek, S. P.; Lynn, D. M. Slippery Liquid-Infused Porous Surfaces That Prevent Microbial Surface Fouling and Kill Non-Adherent Pathogens in Surrounding Media: A Controlled Release Approach. *Adv. Funct. Mater.* **2016,** *26,* 3599-3611.

47. Homeyer, K. H.; Goudie, M. J.; Singha, P.; Handa, H. Liquid-Infused Nitric-Oxide-Releasing Silicone Foley Urinary Catheters for Prevention of Catheter-Associated Urinary Tract Infections. *ACS Biomater. Sci. Eng.* **2019,** *5,* 2021-2029.

48. Carter, M. C. D.; Wong, M. S.; Wang, F.; Lynn, D. M. Influence of Side Chain Hydrolysis on the Evolution of Nanoscale Roughness and Porosity in Amine-Reactive Polymer Multilayers. *Chem. Mater.* **2020,** *32,* 6935-6946.

49. Novick, R. P.; Ross, H. F.; Projan, S. J.; Kornblum, J.; Kreiswirth, B.; Moghazeh, S. Synthesis of Staphylococcal Virulence Factors Is Controlled by a Regulatory Rna Molecule. *The EMBO journal* **1993,** *12,* 3967-3975.

50. Wilsenach, J. A.; Schuurbiers, C. A. H.; van Loosdrecht, M. C. M. Phosphate and Potassium Recovery from Source Separated Urine through Struvite Precipitation. *Water Res.* **2007,** *41,* 458-466.

51. Raguse, T. L.; Porter, E. A.; Weisblum, B.; Gellman, S. H. Structure−Activity Studies of 14-Helical Antimicrobial β-Peptides: Probing the Relationship between Conformational Stability and Antimicrobial Potency. *J. Am. Chem. Soc.* **2002,** *124,* 12774-12785.

52. Porter, E. A.; Weisblum, B.; Gellman, S. H. Use of Parallel Synthesis to Probe Structure−Activity Relationships among 12-Helical β-Peptides: Evidence of a Limit on Antimicrobial Activity. *J. Am. Chem. Soc.* **2005,** *127,* 11516-11529.

53. Buck, M. E.; Zhang, J.; Lynn, D. M. Layer-by-Layer Assembly of Reactive Ultrathin Films Mediated by Click-Type Reactions of Poly(2-Alkenyl Azlactone)s. *Adv. Mater.* **2007,** *19,* 3951-3955.

54. Velraeds, M. M. C.; Van De Belt-Gritter, B.; Van Der Mei, H. C.; Reid, G.; Busscher, H. J. Interference in Initial Adhesion of Uropathogenic Bacteria and Yeasts to Silicone Rubber by a *Lactobacillus Acidophilus* Biosurfactant. *J. Med. Microbiol.* **1998,** *47,* 1081-1085.

55. Papaioannou, T. G.; Stefanadis, C. Vascular Wall Shear Stress: Basic Principles and Methods. *Hellenic. J. Cardiol.* **2005,** *46,* 9-15.

56. Rao, M. A., Application of Rheology to Fluid Food Handling and Processing. In *Rheology of Fluid and Semisolid Foods: Principles and Applications*, Rao, M. A., Ed. Springer US: Boston, MA, 2007; pp 427-469.

57. Goudie, M. J.; Pant, J.; Handa, H. Liquid-Infused Nitric Oxide-Releasing (LINORel) Silicone for Decreased Fouling, Thrombosis, and Infection of Medical Devices. *Sci. Rep.* **2017,** *7,* 13623.

58. Lee, J.; Yoo, J.; Kim, J.; Jang, Y.; Shin, K.; Ha, E.; Ryu, S.; Kim, B.-G.; Wooh, S.; Char, K. Development of Multimodal Antibacterial Surfaces Using Porous Amine-Reactive Films Incorporating Lubricant and Silver Nanoparticles. *ACS Appl. Mater. Interfaces* **2019,** *11,* 6550-6560.

59. Villegas, M.; Alonso-Cantu, C.; Rahmani, S.; Wilson, D.; Hosseinidoust, Z.; Didar, T. F. Antibiotic-Impregnated Liquid-Infused Coatings Suppress the Formation of Methicillin-Resistant *Staphylococcus Aureus* Biofilms. *ACS Appl. Mater. Interfaces* **2021,** *13,* 27774-27783.

For Table of Contents Use Only: